Hindawi Publishing Corporation
Journal of Chemistry
Volume 2013, Article ID 571709, 9 pages
http://dx.doi.org/10.1155/2013/571709

Research Article

Doping the Buckminsterfullerene by Substitution: Density Functional Theory Studies of $C_{59}X$ (X = B, N, Al, Si, P, Ga, Ge, and As)

Hongcun Bai,[1] Wenxin Ji,[1,2] Xiangyu Liu,[1] Liqiong Wang,[1] Nini Yuan,[1] and Yongqiang Ji[1]

[1] *Key Laboratory of Energy Sources and Chemical Engineering, State Key Laboratory Cultivation Base of Natural Gas Conversion, Ningxia University, Ningxia, Yinchuan 750021, China*
[2] *School of Chemistry and Chemical Technology, Shanghai Jiaotong University, Shanghai 200240, China*

Correspondence should be addressed to Hongcun Bai; hongcunbai@gmail.com

Received 13 June 2012; Revised 5 August 2012; Accepted 20 August 2012

Academic Editor: Tatyana E. Shubina

The heterofullerenes $C_{59}X$ (X = B, N, Al, Si, P, Ga, Ge, and As) were investigated by quantum chemistry calculations based on density functional theory. These hybrid cages can be seen as doping the buckminsterfullerene by heteroatom substitution. The geometrical structures, relative stabilities, electronic properties, vibrational frequencies, dielectric constants, and aromaticities of the doped cages were studied systemically and compared with those of the pristine C_{60} cage. It is found that the doped cages with different heteroatoms exhibit various electronic, vibrational, and aromatic properties. These results imply the possibility to modulate the physical properties of these fullerene-based materials by tuning substitution elements.

1. Introduction

Fullerenes and related materials have aroused considerable attention since the discovery of buckminsterfullerene C_{60} [1]. During the last two decades, a great number of studies have been carried out to investigate the structures and physical properties of the carbon cages and the derivates [2–7]. Among various nanostructures derived from fullerenes, the heterofullerenes, in which one or more carbon atoms of the cage are substituted by heteroatoms, have especially caught the eyes of the researchers. The heterofullerenes exhibit unique structural, electronic, and nonlinear optical properties due to the existence of the heteroatom, which are considerably different from those of the pure carbon cages [8–13]. Therefore, heterofullerenes should be interesting new nanoscaled materials to be expected in the future.

In 1991, six years after the experimental discovery of the buckminsterfullerene, Chai et al. [14] claimed the spectroscopic observation of gas-phase formation of heterofullerene ions, indicating that the synthesis of heterofullerenes was achieved. And then, the doped cages obtained by N, B, Si, P, Ge, As, and transition-metal (such as Pt, Fe, and Co) substitution have been reported by several research groups [15–21]. Most recently, N-, P-, and Si- doped single-walled carbon nanotubes (SWCNTs) are also synthesized using chemical vapor deposition method [22].

As for the theoretical side, several literatures have bad attention to the heterofullerenes [9, 11–13, 23–28]. However, most of the studies mainly focus on the geometries and ordinary electronic structures of the doped fullerenes. Up until now a systematic study on the relationship of structure and property for C_{60}-based heterofullerenes by a single approach has not been reported according to our best knowledge. Furthermore, the doped carbon cages are good candidates of materials for hydrogen storage, optical device, and molecular sensor [13, 29, 30], and they have become the state-of-the-art research subjects in recent years. Additionally, the heterofullerenes are of prominent importance since they are the building blocks of various polymerized fullerenes structures [9, 11, 21]. Thus, in order to achieve a further understanding

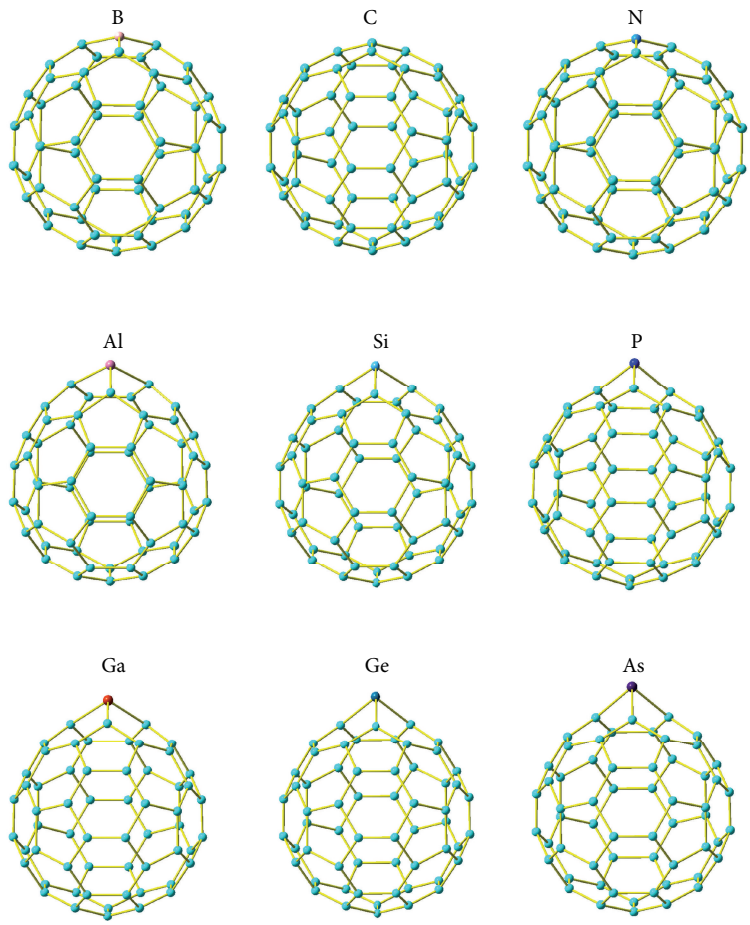

Figure 1: Structures of $C_{59}X$ (X = B, N, Al, Si, P, Ga, Ge, and As) and C_{60} Cages.

of structure-property relationship of carbon cages and the derivates, it is desirable to study heterofullerenes.

In this paper, we carried out systematic calculations on the heterofullerenes obtained by doping C_{60} cage with B, N, Al, Si, P, Ga, Ge and As atoms by means of the Kohn-Sham self-consistent field method under the framework of density functional theory (DFT).

2. Models and Computational Methods

It is known that the synthesized C_{60} have I_h symmetry and all the 60 carbon atoms are equivalent. The heterofullerene structure $C_{59}X$, obtained by only one carbon atom of the C_{60} cage substituted by other atoms, is studied in this paper. The atom of several main group elements, including III (B, Al, and Ga), IV (Si and Ge), and V (N, P, and As) subgroups, are considered as the heteroatom to replace the carbon atom of the buckminsterfullerene cage. The obtained $C_{59}X$ cage only reserves a mirror plane, and the symmetry is reduced to C_s. Different spin states for the doped cages are also considered in our calculations. The ground state is treated as the lowest energy structure.

The DFT hybrid functional B3LYP method [31] is adopted to calculate $C_{59}X$ cages. Both the geometrical optimizations and the electronic property calculations through out this paper are all performed using the Kohn-Sham self-consistent field method at B3LYP/6-31G* level with Gaussian 09 program [32]. In the DFT calculations, symmetry constraint is always adopted, and default values of convergence criteria in Gaussian 09 program are used. According to the previous calculations, the B3LYP method has been successfully applied to the theoretical studies on fullerene-based nanostructres [2–5, 8, 13, 23, 27], and the methods used here could give rather good results compared with those obtained by various different functionals and basis sets [33].

3. Results and Discussion

3.1. Structures. The optimized structures of the $C_{59}X$ (X = B, N, Al, Si, P, Ga, Ge and As) and C_{60} cages are shown in Figure 1, and the bond lengths and atomic coordinates are listed in Tables S1 and S2 (see Supplementary Material available online at doi:http://dx.doi.org/10.1155/2013/571709). From

Table 1: The sphericity parameter (SP), cohesive energy (E_{coh}), ΔE, replacing energy ($E_{replace}$), relaxing energy (E_{relax}) and asphericity parameter (ASP) of C_{60} and the doped cages. (SP in GHz^{-1}; E_{coh} in eV/atom; ΔE, $E_{replace}$ and E_{relax} in eV).

Cages	SP	E_{coh}	ΔE	$E_{replace}$	E_{relax}	ASP
$C_{59}B$	0.126	6.779	−0.932	−0.170	−0.762	0.0045
$C_{59}Al$	1.198	6.697	−1.926	11.839	−13.765	0.0645
$C_{59}Ga$	3.183	6.692	−1.905	13.122	−15.027	0.0659
C_{60}	0.000	6.813	0.000	0.000	0.000	0.0000
$C_{59}Si$	1.169	6.733	−1.373	7.958	−9.331	0.0509
$C_{59}Ge$	3.546	6.724	−1.437	12.550	−13.987	0.0685
$C_{59}N$	0.055	6.807	0.020	0.144	−0.124	0.0013
$C_{59}P$	1.273	6.759	−1.235	6.879	−8.114	0.0502
$C_{59}As$	3.637	6.753	−1.402	13.273	−14.675	0.0736

Figure 1 we can see that all the doped cages undergo some distortions due to the heteroatoms, though they still preserve closed cage structures. Here to evaluate the sphericity of the doped cages, the sphericity parameter (SP) is calculated through the equation [34, 35]:

$$\mathrm{SP} = \left[\left(\frac{1}{A} - \frac{1}{B}\right)^2 + \left(\frac{1}{A} - \frac{1}{C}\right)^2 + \left(\frac{1}{B} - \frac{1}{C}\right)^2\right]^{1/2}, \quad (1)$$

where A, B, and C are the rotational constants (in GHz) of the corresponding cages. The structure with larger SP value is distorted more away from perfect sphere. As shown in Table 1, SP of C_{60} is zero, and it comes without surprise because C_{60} with I_h symmetry has the perfect sphere shape. As for the doped cages, the values of SP are in the range of 0.055–3.637 GHz^{-1}, indicating that deformations of the cage are occurred when the heteroatom is introduced into the pristine cage. It can be seen that SP are about 0.1 GHz^{-1} for $C_{59}X$ with X = B and N, while about 1.2 GHz^{-1} for X = Al, Si, and P, and the values of SP are even larger than 3.1 GHz^{-1} for X = Ga, Ge, and As. Thus, it is clearly that the cage with larger heteroatom gives larger SP and more obvious distortion.

Then we pay attention to the bond lengths of the heterofullerenes. It is well-known that there are two kinds of C–C bond in C_{60} cage, the [6, 6] bond and the [5, 6] bond. The bond lengths are 1.395 and 1.454 Å for [6, 6] and [5, 6] bonds, respectively, based on our DFT calculations, which agree well with 1.391 (or 1.39) and 1.455 (or 1.46) Å by neutron diffraction experiments [36, 37]. When the carbon cage is doped by the heteroatom, the C–X bonds are presented. From Table S1, it can be seen that the C–X bond lengths are in the range of 1.404–1.950 Å. The bond lengths increased obviously for X = B, Al, Si, P, Ga, Ge, and As, ranking from 1.526 Å to 1.950 Å. However, the C–N bonds in $C_{59}N$ are 1.408 and 1.424 Å, and thus the original [5, 6] bond is even decreased by 0.03 Å compared with that in the pristine cage. It is also found that the C–X bond lengths increase more significantly for the larger heteroatoms. For instance, the C–B bonds are 1.526 and 1.549 Å, while the C–X bonds (X = Al, Si, P) are calculated to be within 1.796–1.904 Å, but the values are even 1.876–1.950 Å for X = Ga, Ge, As. These results also agree with our SP analyses as well as the previous studies [25–28]. Now we focus on the C–C bonds in the doped fullerenes. As shown in Table S1, the original [6, 6] and [5, 6] bonds exhibit slight changes, with the lengths in the range of 1.385–1.427 Å and 1.433–1.517 Å, respectively. Moreover, it also can be seen that the C–C bond lengths change more significantly near the region of the heteroatom, but almost inert in the region away from the heteroatom.

3.2. Energies and Relative Stabilities. The doped cages with different spin-multiplicity states are calculated with open-shell DFT B3LYP/6-31G* method to determine the ground state, and their energies are listed in Table S3 of supplementary material. It can be seen that the high-spin state structures always exhibit higher energies than those of the low-spin states according to the obtained energies (both corrected and uncorrected with zero-point vibrational energies). Thus, the spin multiplicity of the ground state of $C_{59}X$ is 1 for IV group elements, and 2 for III and V elements, respectively.

In order to study the thermodynamic stabilities of the doped cages, the cohesive energy (E_{coh}) per atom are calculated with the energies corrected with zero-point energy (ZPE), and the obtained results are listed in Table 1 and shown in Figure 2(a). Here the system with larger E_{coh} is more stable. We can see that E_{coh} of C_{60} is calculated to be 6.813 eV/atom, and agrees with the previous results [9, 38]. E_{coh} of the heterofullerene cages are in the range of 6.692–6.807 eV/atom, and slightly smaller than those of the pristine cage. Thus the introduced heteroatoms would decrease the thermodynamic stability of the cages from viewpoint of cohesive energy. From Figure 2(a), we can see that E_{coh} of $C_{59}X$ with X = B and N are larger than those of $C_{59}X$ with X = Al, Si, P, and even a bit more larger than those of $C_{59}X$ with X = Ga, Ge, and As. Therefore, the doped cage with smaller heteroatom is more stable.

The formation of the $C_{59}X$ cage can be seen in reaction (2).

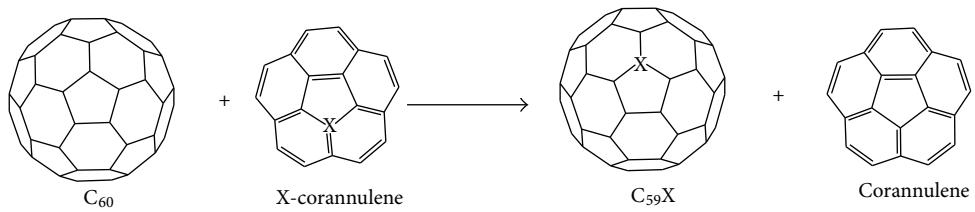

(2)

Then the energy difference of the above process, ΔE, can be calculated by:

$$\Delta E = E\left(C_{59}X\right) + E\left(\text{corannulene}\right) - E\left(C_{60}\right) - E\left(\text{X-corannulene}\right), \tag{3}$$

where $E(C_{59}X)$, $E(C_{60})$, E(corannulene) and E(X-corannulene), are the energies of the species with the minimum structure, respectively. Furthermore, from theoretical point of view, the formation reaction of $C_{59}X$ cage from C_{60} cage can be considered as two processes. In the first step, one carbon atom of the carbon cage is directly replaced by the heteroatom from the doped corannulene to form a hybrid structure, for which the skeleton of the hybrid cage is still the same as that of the pristine C_{60} cage. In the next step the hybrid cage is then relaxed to reach its minimum structure. Therefore, the replacing energy (E_{replace}) and the relaxing energy (E_{relax}) for the two processes are defined as follows:

$$\begin{aligned} E_{\text{replace}} &= E\left(C_{59}X^{*}\right) + E\left(\text{corannulene}\right) \\ &\quad - E\left(C_{60}\right) - E\left(\text{X-corannulene}\right), \\ E_{\text{relax}} &= E\left(C_{59}X\right) - E\left(C_{59}X^{*}\right), \end{aligned} \tag{4}$$

where $E(C_{59}X^{*})$ is the energy of a $C_{59}X$ cage with the skeleton the same as that of the pristine C_{60} cage. Based on (3)-(4), it is easy to get $\Delta E = E_{\text{replace}} + E_{\text{relax}}$. The calculated ΔE, E_{replace}, and E_{relax} are shown in Table 1 and Figures 2(b)–2(d).

We can see that ΔE of the doped cages are all negative except for that of $C_{59}N$, indicating the formations of the most doped cages are exothermic. Even for $C_{59}N$, the obtained ΔE is only 0.020 eV. Thus it is energetically favorable to form the $C_{59}X$ cages from viewpoint of total energy change. The obtained ΔE are ranged from −1.926 to 0.020 eV for the heterofullerenes studied in this paper. From Figure 2(b), we can see that the curves of ΔE have the same trend as those of the E_{coh}. Thus, contrary to the cohesive energy results, it seems that the formation of the doped cage with larger heteroatom is energetically more favorable from viewpoint of the total energy change of the reaction.

As for E_{replace} of the heterofullerenes, $C_{59}B$ gives −0.170 eV, but others all exhibit positive values in the range of 0.144–13.273 eV. This fact means that the directly replacement of a carbon atom by a heteroatom is an endoergic process for most of the doped cages. From Figure 2(c) for E_{replace} of $C_{59}X$ where X belongs to III, IV and V Groups, it can be seen that E_{replace} decrease monotonically for each group. Furthermore, E_{replace} of $C_{59}B$ and $C_{59}N$ are the smallest among the eight doped cages studied in this paper. This is because the C–B and C–N bond lengths are more close to that of the C–C bond compared with those of other C–X bonds. Thus $C_{59}N$ has the least E_{replace}, and $C_{59}B$ even exhibits exothermic replace process.

Now we turn to the relaxing energy, E_{relax}. From the obtained E_{relax} shown in Table 1 and Figure 2(d), it can be seen that all obtained E_{relax} of the doped cages are negative, indicating that the relaxing effect is exothermic. The calculated E_{relax} are ranged from −0.124 to −15.027 eV for the heterofullerenes.

Since the doped cage becomes distorted structure from a perfect ball in the relaxing process, the asphericity parameter, ASP, is calculated to evaluate the geometrical distortion for the doped cages. ASP is introduced by Fowler et al. and can be calculated by [39]:

$$\text{ASP} = \sum \frac{\left(R_i - R_0\right)^2}{{R_0}^2}, \tag{5}$$

where R_i is the radial distance of atom i from the cage central of mass, and R_0 is the average radius. Here the structures with smaller ASP values are more close to a perfect sphere shape. The obtained ASP is listed in Table 1. It can be seen that the calculated ASP are all nonzero for the heterofullerenes, with the values in the range of 0.001–0.074. This result also confirms the distortions of the cage away from the perfect sphere. Furthermore, it seems that ASP of the cages has something to do with E_{relax}. Here the doped cage with larger ASP values gives more negative E_{relax}. For instance, $C_{59}N$ and $C_{59}B$ have the smallest ASP (less than 0.005) and the E_{relax} are only −0.124 and −0.762 eV, respectively. $C_{59}Si$ and $C_{59}P$ have larger ASP (about 0.05) and the E_{relax} are also more negative (about −8 and −9 eV). For $C_{59}Al$, $C_{59}Ga$, $C_{59}Ge$, and $C_{59}As$, they have the largest ASP (larger than 0.065) and also the most negative E_{relax} (less than −13 eV).

3.3. Electronic Properties. It is well-known that the frontier orbitals, the highest occupied molecular orbital (HOMO), and the lowest unoccupied molecular orbital (LUMO) play

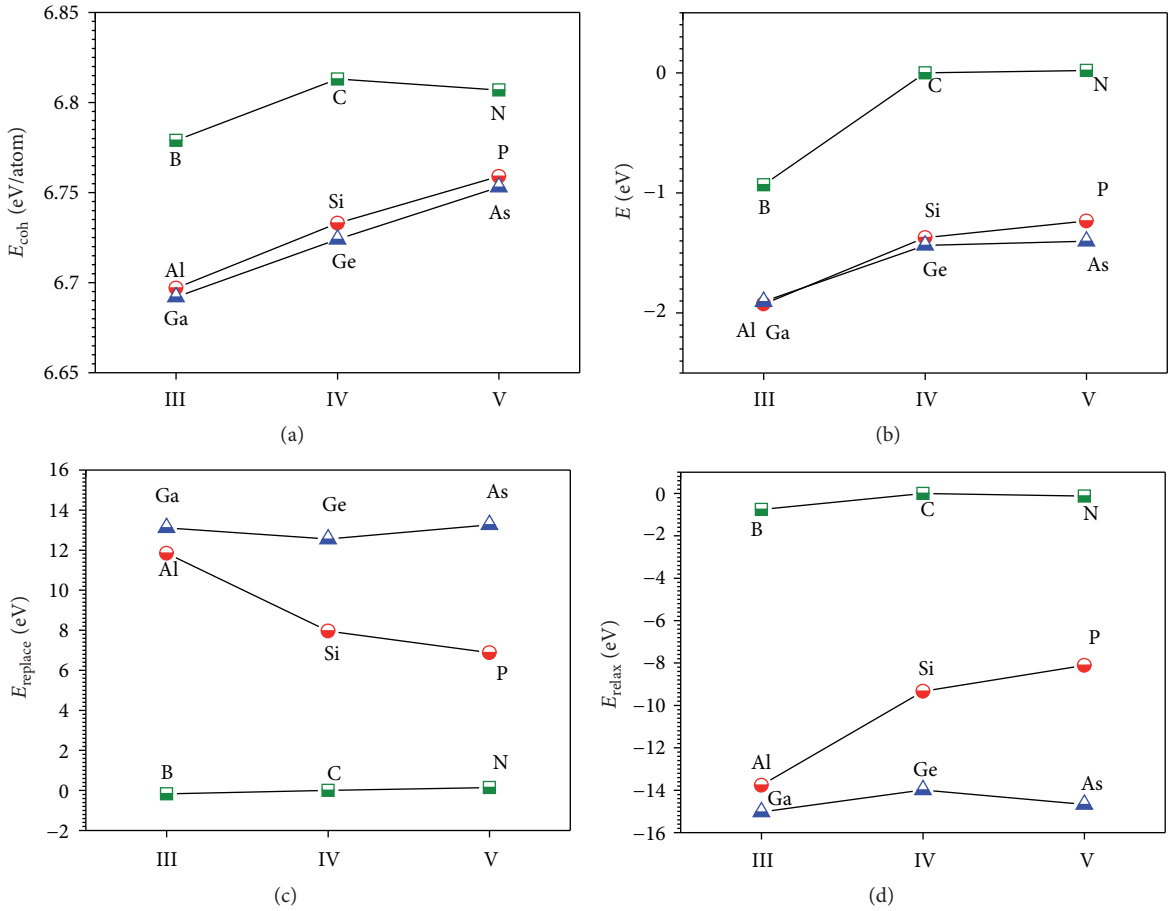

FIGURE 2: The obtained energies of the doped and pristine carbon cages. (a) E_{coh}; (b) ΔE; (c) $E_{replace}$ and (d) E_{relax}.

an important role in chemical reaction for the reactant molecule, thus the frontier orbital analysis of the doped cages is necessary. In Table 2, we summarize the HOMO and LUMO energy levels of the heterofullerenes. It can be seen that HOMO levels of the doped cages are all increased compared with that of C_{60}. However, the HOMO levels all vary not very large, except for that of $C_{59}N$, which is increased by 1.4 eV. As for LUMO levels, they are decreased by about 0.5 eV when doping with Si and Ge atoms, but nearly unchanged for doping with other atoms compared with that of the pristine cage.

Figure S2 in Supplementary Material shows the distributions of HOMO and LUMO for the cages studied in this paper. It can be seen that the frontier orbitals of C_{60} cage are rather delocalized and spread over the whole surface of the cage. However, the frontier orbitals of several doped cages become localized obviously due the present of the heteroatoms. For example, the contributions from the Si, Ga, and Ge atoms are as large as 27.4%, 16.4%, and 35.3% to the HOMO, while 24.3%, 42.6% and 22.4% to LUMO, respectively according to our quantitative evaluations.

It is known that both the thermodynamic stability and kinetic stability have crucial influence on the relative abundances of different fullerene structures. It has been pointed out that higher kinetic stability is usually related with a larger HOMO-LUMO energy gap (E_g) [40], because exciting electrons from a low HOMO to a high LUMO is energetically unfavorable, which would be necessary to activate a reaction. The calculated E_g of the doped cages are listed in Table 2. It can be found that all the doped cages present smaller E_g than that of C_{60} cage. Thus kinetic stability of the cage is decreased by substitution from viewpoint of HOMO-LUMO gap.

Since the charge transport is one of the central issues for the performance of organic electronic devices, here the exciton binding energy (E_b) is calculated to understand more about the transport properties of the doped fullerenes. Physically, the exciton binding energy can be seen as the energy required to decompose an exciton into a free electron and hole in the solid, and is defined as follows:

$$E_b = E_t - E_{opt}, \tag{6}$$

where E_t is the transport gap and E_{opt} is the optical gap. E_t can be treated as the orbital energy difference between the LUMO and the HOMO [41]. As for E_{opt}, it is calculated to be as the allowed lowest singlet optical transition energy with nonzero oscillator strength obtained by the time-dependent DFT (TD-DFT) calculations at B3LYP/6-31G* theory level in this paper. Here the obtained E_{opt} of C_{60} is 2.099 eV, which agrees with 1.95 eV by experiment of optical absorption spectrum

Table 2: The obtained HOMO, LUMO, E_g, E_{opt}, E_b, α, υ, ε and NICS of C_{60} and the doped cages (HOMO, LUMO, E_g, E_{opt} and E_b in eV, and α and υ in Å^3).

Cages	HOMO	LUMO	E_g	E_{opt}	E_b	α	υ	ε	NICS
$C_{59}B$	−5.660	−3.225	2.435	0.807	1.629	71.75	631.96	3.72	−5.94
$C_{59}Al$	−5.377	−3.120	2.257	1.018	1.239	75.48	640.92	3.92	−5.62
$C_{59}Ga$	−5.442	−3.240	2.202	0.964	1.238	75.77	640.09	3.95	−5.65
C_{60}	−5.988	−3.223	2.765	2.099	0.666	69.45	622.93	3.63	−2.72
$C_{59}Si$	−5.817	−3.649	2.168	1.646	0.523	74.98	641.32	3.88	−2.80
$C_{59}Ge$	−5.887	−3.769	2.118	1.509	0.608	75.81	648.08	3.88	−3.18
$C_{59}N$	−4.584	−3.295	1.290	0.664	0.626	71.38	616.53	3.82	−2.41
$C_{59}P$	−5.202	−3.252	1.950	1.275	0.675	73.12	632.85	3.81	−4.85
$C_{59}As$	−5.247	−3.220	2.027	1.339	0.688	73.70	637.16	3.82	−5.25

[42] and 2.31 eV calculated by the UNO-CIS method [43, 44]. Then 2.765 minus 2.099 eV gives E_b of C_{60} cage with 0.666 eV. From Table 2, we can see that E_b of the $C_{59}X$ cage with X to be IV and V Groups are in the range of 0.523–0.688 eV, which are very close to that of the C_{60}. However, $C_{59}X$ with X = B, Al and Ga exhibit obvious larger E_b (1.629, 1.239 and 1.238 eV, resp.). Thus compared with C_{60} and other heterofullerenes, more energy is required to decompose the exciton for the cages doped with III Group elements. Therefore, it seems that the charge transport behaviors would be quite different for the hole-type doped buckminsterfullerenes considering the exciton binding energy.

3.4. Vibrational Frequencies and Infrared Spectrum. Based on the DFT calculations, the vibrational frequency analysis is performed with B3LYP/6-31G* method to verify whether these doped cages are local minima on the potential energy surface. The calculated vibrational frequencies for all the cages show no imaginary vibrational frequency, indicating that these doped structures all correspond to the true minima on the potential energy surface.

The obtained infrared (IR) spectra were simulated as plotted in Figure 3, which have been scaled by a factor of 0.98, according to the DFT study on the infrared spectra of fullerene structures [45]. From Figure 3 we can see that there are four IR-active absorptions at 530, 575, 1188, and 1431 cm^{-1}, respectively, for the C_{60} cage. It is because only four F_{1U} vibrational models are IR allowed by symmetry, though the perfect C_{60} with I_h symmetry has 174 models totally. Our results agree quite well with the experimental (528, 577, 1183, and 1429 cm^{-1}) [46] and other DFT results [47, 48]. As for the doped cages, their IR spectra are more complicated. It is found that the original four peaks are split and more absorptions are present. These absorptions all exhibit somewhat red or blue shift due to the substitution of the heteroatoms compared with those of the pristine cage. Furthermore, it can be see that there are also several new peaks in the region of 600–1100 cm^{-1}. This is because the symmetry of the doped cages is decreased from I_h to C_s, and thus some of the original vibrational models forbidden by symmetry become IR-active. Additionally, it can be seen that the shapes of IR absorption spectra are different for the different doped cages. These characteristic features in the IR spectra could be helpful to identify these heterofullerens from the experimental spectra.

3.5. Dielectric Constant. The dielectric constant is one of the important parameters for the materials of organic solid. In this paper a simple model based on the Clausius-Mossotti equation [49] is adopted. This model has been used to successfully evaluate the dielectric constant of C_{60} and conjugated organic molecules [49, 50]. Under the framework of the Clausius-Mossotti model, the dielectric constant, ε, can be expressed as:

$$\varepsilon = \frac{1 + 8\pi\alpha/3\upsilon}{1 - 4\pi\alpha/3\upsilon}, \tag{7}$$

where α is the first order polarizability with $\alpha = (1/3)\sum \alpha_{ii}$, in which α_{ii} are the diagonal matrix elements of the tensor. υ is the volume occupied by a single molecule (tight option was taken for better accuracy). ε of C_{60} is calculated to be 3.63 in this paper, which is comparable with previous experimental [51] and theoretical results [49]. From Table 2, we can see that ε of the doped cages are in the range of 3.72–3.95. Thus the substituted doping could increase ε of the cages. It is also found that for $C_{59}X$ cage $\alpha$is increase by 2.8–9.2% by substituted doping compared with that of C_{60}. However, doping with N atom even decreased υ by 1.0%, and for other heteroatoms υ is only increased by 1.5–4.0%. Recall that larger ε is related with larger α and smaller υ values according to (7). As a result, all the doped cages exhibit larger dielectric constant than that of C_{60}.

3.6. Aromaticity and Nuclear Independent Chemical Shift. Aromaticity can be explained by the ring current theory and is a significant concept in chemistry. In this paper the aromaticity of the cages is evaluated by using the nuclear independent chemical shift (NICS), which has proven to be a simple and efficient aromaticity probe [52–54]. The NICS is defined as the negative of the isotropic magnetic shielding constant of a ghost atom located at the central of the cage. Negative NICS value means the aromaticity of the cage. In

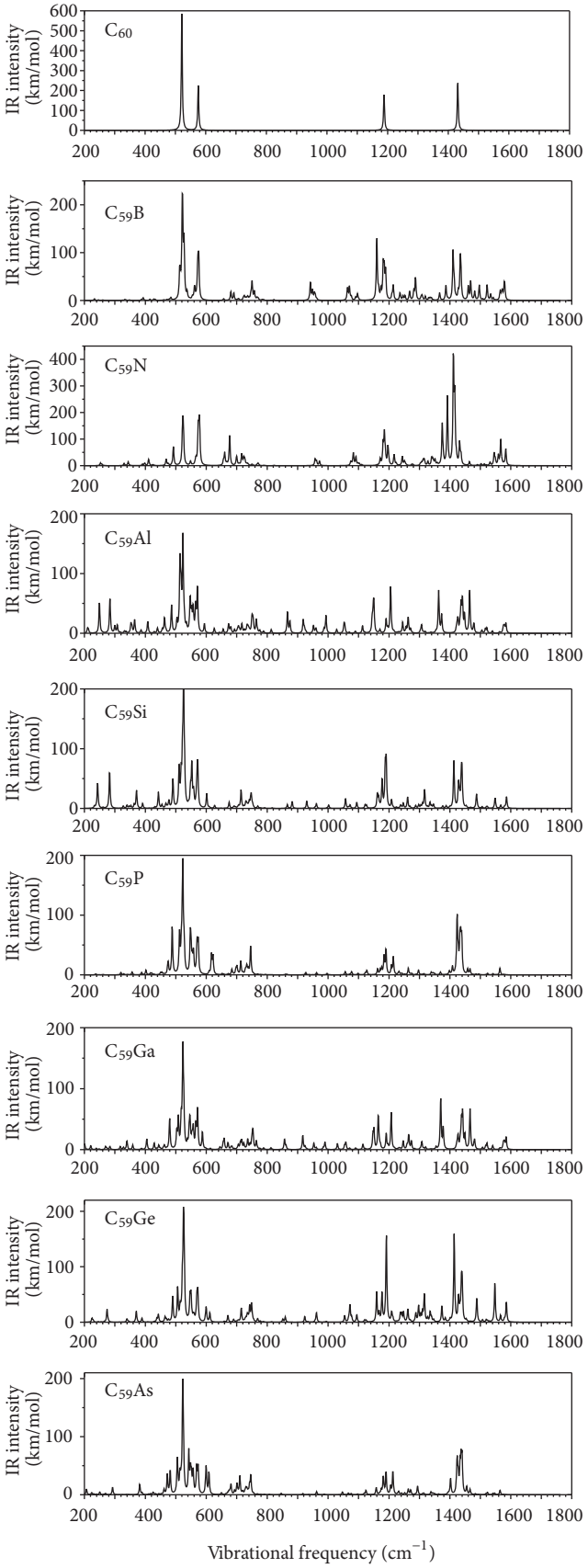

Figure 3: The claculated IR spectra of C_{60} and the doped cages.

this study, the NICS values listed in Table 2 is computed with the gauge-including atomic orbital (GIAO) method at B3LYP/6-31G* theory level. NICS of C_{60} we obtained is −2.72, which indicates the weak aromaticity of C_{60} and also agrees well with −2.8 by previous DFT calculation [55]. From Table 2, it can be seen that all the doped cages in this paper give negative NICS. Thus the eight doped cages studied are all aromatic. Among them, $C_{59}N$ cage has the NICS of −2.41, indicating it is slightly less aromatic than C_{60}. As for other doped cages, the obtained NICS are more negative and thus they are more aromatic than the pristine cage, though the difference is small. Additionally, the $C_{59}B$ cage gives the most negative NICS, though it is only a bit distorted from the perfect sphere shape according to the SP and ASP analysis. Therefore, it seems that there is no uniform correlation between the aromaticity and the sphere shape for the doped fullerenes.

Since it has been pointed that NICS at the cage centers have essentially the same values as the endohedral helium chemical shifts [55, 56], these obtained values are also helpful for the possible characterization of these doped fullerene cages.

4. Conclusion

Theoretical studies of the $C_{59}X$ (X = B, N, Al, Si, P, Ga, Ge, and As) have been performed systemically based on the DFT calculations. The results of the geometrical structures, relative stabilities, electronic properties, vibrational frequencies, dielectric constants, and the aromaticities of the doped cages were discussed to achieve a further understanding of structure-property relationship of the doped cages. It is found that the hybrid cages undergo some distortions due to the substitution of the heteroatoms. According to the calculated cohesive energies, the $C_{59}X$ cage with smaller heteroatom is more stable. HOMOs of the heterofullerenes are all increased, but the HOMO-LUMO gaps are decreased compared with those of the C_{60}. As for the exciton binding energy, the cages doped with III Group elements are obviously larger than other cages. The calculations also indicate that doping C_{60} by substitution would give larger dielectric constant due to the increased polarizability. The obtained NICS show that most of the doped fullerenes are lightly more aromatic than the pristine cage. However, no correlation between the aromaticity and the sphere shape is found for the doped cages.

Acknowledgments

This work is supported by Scientific Research Foundation of Ningxia University (no. ZR1150 and ZR1151), Natural Science Foundation of Ningxia (no. NZ12136), National Natural Science Foundation of China (no. 21064005, 21266023, and 21263020), 973 Program of China (no. 2010CB534916 and 2012CB723106), and 2011 Research Foundation of Ningxia High Education and Universities. The High Performance Computer Center of Ningxia University is appreciated for providing computational resources.

References

[1] H. W. Kroto, J. R. Heath, S. C. O'Brien, R. F. Curl, and R. E. Smalley, "C_{60}: buckminsterfullerene," *Nature*, vol. 318, no. 6042, pp. 162–163, 1985.

[2] D. Wang, H. Xu, Z. Su, and D. Hou, "Ab initio and density functional study on fullerene C_{44} and its derivatives," *Computational and Theoretical Chemistry*, vol. 978, no. 1–3, pp. 166–171, 2011.

[3] D. Wang, X. Wang, X. Gao, and D. Hou, "Theoretical study on the interaction of oxygen atom with C_{90} (D_{5h})," *Computational and Theoretical Chemistry*, vol. 989, pp. 33–38, 2012.

[4] H. Bai, R. Du, W. Qiao, and Y. Huang, "Structures, stabilities and electronic properties of C_{50} dimers," *Journal of Molecular Structure: THEOCHEM*, vol. 961, no. 1–3, pp. 42–47, 2010.

[5] H. Bai, Y. Ai, and Y. Huang, "Theoretical studies of one-dimensional C_{36} coplanar polymers," *Physica Status Solidi B*, vol. 248, no. 4, pp. 969–973, 2011.

[6] H. Bai, W. Qiao, Y. Zhu, and Y. Huang, "Theoretical study on one-dimensional C_{50} polymers," *Diamond and Related Materials*, vol. 26, pp. 20–24, 2012.

[7] X. Lu and Z. Chen, "Curved Pi-conjugation, aromaticity, and the related chemistry of small fullerenes ($<C_{60}$) and single-walled carbon nanotubes," *Chemical Reviews*, vol. 105, no. 10, pp. 3643–3696, 2005.

[8] F. L. Liu, "Heterofullerene molecules $C_{58}X$ (X = S, Se, Te): a DFT study," *Chemical Physics Letters*, vol. 471, no. 1–3, pp. 116–121, 2009.

[9] J. Li, Y. Xia, M. Zhao et al., "From pure C60 to silicon carbon fullerene-based nanotube: an ab initio study," *Journal of Chemical Physics*, vol. 128, no. 15, Article ID 154719, 8 pages, 2008.

[10] M. N. Huda and A. K. Ray, "Evolution of SiC nanocluster from carbon fullerene: a density functional theoretic study," *Chemical Physics Letters*, vol. 457, no. 1–3, pp. 124–129, 2008.

[11] P. A. Marcos, J. A. Alonso, and M. J. López, "Stability of silicon-doped C_{60} dimers," *Journal of Chemical Physics*, vol. 126, no. 4, Article ID 044705, 6 pages, 2007.

[12] X. Xu and H. S. Kang, "Computational evidence for the possible existence of the open heterofullerenes $C_{56}X_2Y$ (X = N, P; Y = O, S) and $C_{60-6k}N_{4k}$," *Chemical Physics Letters*, vol. 441, no. 4–6, pp. 300–304, 2007.

[13] R. H. Xie, L. Jensen, G. W. Bryant, J. Zhao, and V. H. Smith Jr., "Structural, electronic, and magnetic properties of heterofullerene $C_{48}B_{12}$," *Chemical Physics Letters*, vol. 375, no. 5-6, pp. 445–451, 2003.

[14] Y. Chai, T. Guo, C. Jin et al., "Fullerenes with metals inside," *Journal of Physical Chemistry*, vol. 95, no. 20, pp. 7564–7568, 1991.

[15] T. Pradeep, V. Vijayakrishnan, A. K. Santra, and C. N. R. Rao, "Interaction of nitrogen with fullerenes: nitrogen derivatives of C_{60} and C_{70}," *Journal of Physical Chemistry*, vol. 95, no. 26, pp. 10564–10565, 1991.

[16] J. L. Fye and M. F. Jarrold, "Structures of silicon-doped carbon clusters," *Journal of Physical Chemistry A*, vol. 101, no. 10, pp. 1836–1840, 1997.

[17] H. J. Muhr, R. Nesper, B. Schnyder, and R. Kötz, "The boron heterofullerenes $C_{59}B$ and $C_{69}B$: generation, extraction, mass spectrometric and XPS characterization," *Chemical Physics Letters*, vol. 249, no. 5-6, pp. 399–405, 1996.

[18] C. Möschel and M. Jansen, "Darstellung stabiler Phosphor-Heterofullerene im Hochfrequenzofen," *Zeitschrift für Anorganische und Allgemeine Chemie*, vol. 625, pp. 175–177, 1999.

[19] W. Branz, I. M. L. Billas, N. Malinowski, F. Tast, M. Heinebrodt, and T. P. Martin, "Cage substitution in metal-fullerene clusters," *Journal of Chemical Physics*, vol. 109, no. 9, pp. 3425–3430, 1998.

[20] J. M. Poblet, J. Muñoz, K. Winkler et al., "Geometric and electronic structure of metal-cage fullerenes, $C_{59}M$ (M = Pt, Ir) obtained by laser ablation of electrochemically deposited films," *Chemical Communications*, vol. 30, no. 23, 1999.

[21] O. Vostrowsky and A. Hirsch, "Heterofullerenes," *Chemical Reviews*, vol. 106, no. 12, pp. 5191–5207, 2006.

[22] J. Campos-Delgado, I. O. Maciel, D. A. Cullen et al., "Chemical vapor deposition synthesis of N-, P-, and Si-doped single-walled carbon nanotubes," *ACS Nano*, vol. 4, no. 3, pp. 1696–1702, 2010.

[23] J. Lu, Y. Zhou, Y. Luo, Y. Huang, X. Zhang, and X. Zhao, "Structural and electronic properties of heterofullerene $C_{59}P$," *Molecular Physics*, vol. 99, no. 14, pp. 1203–1207, 2001.

[24] J. Lu, Y. Luo, Y. Huang, X. Zhang, and X. Zhao, "Semiempirical calculations on heterofullerene $C_{59}Si$: structural and electronic localization," *Solid State Communications*, vol. 118, no. 6, pp. 309–312, 2001.

[25] I. M. L. Billas, C. Massobrio, M. Boero et al., "First principles calculations of Si doped fullerenes: structural and electronic localization properties in $C_{59}Si$ and $C_{58}Si_2$," *Journal of Chemical Physics*, vol. 111, no. 15, pp. 6787–6796, 1999.

[26] H. Jiao, Z. Chen, A. Hirsch, and W. Thiel, "Structures and magnetic properties of mono-doped fullerenes $C_{59}X_n$ and $C_{59}X^-_{(6-n)}$ (X = B^-, N^+, P^+, As^+, Si): isoelectronic analogues of C_{60} and C_{60}^{6-}," *Journal of Molecular Modeling*, vol. 9, no. 1, pp. 34–38, 2003.

[27] T. M. Simeon, I. Yanov, and J. Leszczynski, "Ab initio quantum chemical studies of fullerene molecules with substitutes $C_{59}X$ [X = Si, Ge, Sn], $C_{59}X^-$ [X = B, Al, Ga, In], and $C_{59}X^+$ [X = N, P, As, Sb]," *International Journal of Quantum Chemistry*, vol. 105, no. 4, pp. 429–436, 2005.

[28] L. Koponen, M. J. Puska, and R. M. Nieminen, "Photoabsorption spectra of small fullerenes and Si-heterofullerenes," *Journal of Chemical Physics*, vol. 128, no. 15, Article ID 154307, 7 pages, 2008.

[29] Q. Sun, Q. Wang, and P. Jena, "Functionalized heterofullerenes for hydrogen storage," *Applied Physics Letters*, vol. 94, no. 1, Article ID 013111, 3 pages, 2009.

[30] E. Zahedi and A. Seif, "Adsorption of NH_3 and NO_2 molecules on $C_{48}B_6N_6$ heterofullerene: a DFT study on electronic properties," *Physica B*, vol. 406, no. 19, pp. 3704–3709, 2011.

[31] A. D. Becke, "Density-functional thermochemistry. III. The role of exact exchange," *The Journal of Chemical Physics*, vol. 98, no. 7, pp. 5648–5652, 1993.

[32] M. J. Frisch, G. W. Trucks, H. B. Schlegel et al., *Gaussian 09*, Gaussian, Wallingford, Conn, USA, 2009.

[33] P. O. Dral, T. E. Shubina, A. Hirsch, and T. Clark, "Influence of electron doping on the hydrogenation of fullerene C_{60}: a theoretical investigation," *ChemPhysChem*, vol. 12, no. 14, pp. 2581–2589, 2011.

[34] S. Díaz-Tendero, F. Martín, and M. Alcamí, "Structure and electronic properties of fullerences C_{52}^{q+}: is C_{52}^{2+} an exception to the pentagon adjacency penalty rule?" *ChemPhysChem*, vol. 6, no. 1, pp. 92–100, 2005.

[35] S. Díaz-Tendero, M. Alcamí, and F. Martín, "Fullerene C_{50}: sphericity takes over, not strain," *Chemical Physics Letters*, vol. 407, no. 1–3, pp. 153–158, 2005.

[36] F. Li, D. Ramage, J. S. Lannin, and J. Conceicao, "Radial distribution function of C_{60}: structure of fullerene," *Physical Review B*, vol. 44, no. 23, pp. 13167–13170, 1991.

[37] W. I. F. David, R. M. Ibberson, J. C. Matthewman et al., "Crystal structure and bonding of ordered C_{60}," *Nature*, vol. 353, no. 6340, pp. 147–149, 1991.

[38] H. Bai, Y. Zhu, W. Qiao, and Y. Huang, "Structures, stabilities and electronic properties of graphdiyne nanoribbons," *RSC Advances*, vol. 1, pp. 768–775, 2011.

[39] P. W. Fowler, T. Heine, and F. Zerbetto, "Competition between even and odd fullerenes: C_{118}, C_{119}, and C_{120}," *Journal of Physical Chemistry A*, vol. 104, no. 42, pp. 9625–9629, 2000.

[40] J. I. Aihara, "Weighted HOMO-LUMO energy separation as an index of kinetic stability for fullerenes," *Theoretical Chemistry Accounts*, vol. 102, no. 1–6, pp. 134–138, 1999.

[41] P. I. Djurovicha, E. I. Mayob, S. R. Forrestc, and M. E. Thompsona, "Measurement of the lowest unoccupied molecular orbital energies of molecular organic semiconductors," *Organic Electronics*, vol. 10, no. 3, pp. 515–520, 2009.

[42] H. Ajie, M. M. Alvarez, S. J. Anz et al., "Characterization of the soluble all-carbon molecules C_{60} and C_{70}," *Journal of Physical Chemistry*, vol. 94, no. 24, pp. 8630–8633, 1990.

[43] P. O. Dral and T. Clark, "Semiempirical UNO-CAS and UNO-CI: method and applications in nanoelectronics," *The Journal of Physical Chemistry A*, vol. 115, no. 41, pp. 11303–11312, 2011.

[44] M. Salinas, C. M. Jäger, A. Y. Amin et al., "The relationship between threshold voltage and dipolar character of self-assembled monolayers in organic thin-film transistors," *Journal of the American Chemical Society*, vol. 134, no. 30, pp. 12648–12652, 2012.

[45] R. E. Stratmann, G. E. Scuseria, and M. J. Frisch, "Density functional study of the infrared vibrational spectra of C_{70}," *Journal of Raman Spectroscopy*, vol. 29, no. 6, pp. 483–487, 1998.

[46] W. Kratschmer, L. D. Lamb, K. Fostiropoulos, and D. R. Huffman, "Solid C_{60}: a new form of carbon," *Nature*, vol. 347, no. 6291, pp. 354–358, 1990.

[47] J. Fabian, "Theoretical investigation of the C_{60} infrared spectrum," *Physical Review B*, vol. 53, no. 20, pp. 13864–13870, 1996.

[48] K. Esfarjani, Y. Hashi, J. Onoe, K. Takeuchi, and Y. Kawazoe, "Vibrational modes and IR analysis of neutral photopolymerized C_{60} dimers," *Physical Review B*, vol. 57, no. 1, pp. 223–229, 1998.

[49] P. E. Schwenna, P. L. Burnb, and B. J. Powella, "Calculation of solid state molecular ionisation energies and electron affinities for organic semiconductors," *Organic Electronics*, vol. 12, no. 2, pp. 394–403, 2011.

[50] P. K. Nayak and N. Periasamy, "Calculation of electron affinity, ionization potential, transport gap, optical band gap and exciton binding energy of organic solids using "solvation" model and DFT," *Organic Electronics*, vol. 10, no. 7, pp. 1396–1400, 2009.

[51] P. C. Eklund, A. M. Rao, Y. Wang et al., "Optical properties of C_{60} and C_{70}-based solid films," *Thin Solid Films*, vol. 257, no. 2, pp. 211–232, 1995.

[52] P. V. R. Schleyer, C. Maerker, A. Dransfeld, H. Jiao, and N. J. R. van Eikema Hommes, "Nucleus-independent chemical shifts: a simple and efficient aromaticity probe," *Journal of the American Chemical Society*, vol. 118, no. 26, pp. 6317–6318, 1996.

[53] P. R. Schleyer, H. Jiao, N. J. R. E. Hommes, V. G. Malkin, and O. L. Malkina, "An evaluation of the aromaticity of inorganic rings: refined evidence from magnetic properties," *Journal of the American Chemical Society*, vol. 119, pp. 2669–12670, 1997.

[54] M. Murata, Y. Ochi, F. Tanabe, K. Komatsu, and Y. Murata, "Internal magnetic fields of dianions of fullerene C_{60} and its cage-opened derivatives studied with encapsulated H_2 as an NMR probe," *Angewandte Chemie—International Edition*, vol. 47, no. 11, pp. 2039–2041, 2008.

[55] Z. Chen and R. B. King, "Spherical aromaticity: recent work on fullerenes, polyhedral boranes, and related structures," *Chemical Reviews*, vol. 105, no. 10, pp. 3613–3642, 2005.

[56] Z. Chen, J. Cioslowski, N. Rao et al., "Endohedral chemical shifts in higher fullerenes with 72–86 carbon atoms," *Theoretical Chemistry Accounts*, vol. 106, no. 5, pp. 364–368, 2001.